Body-wave attenuation near the rupture of the 1887 Sonora, México, earthquake (Mw 7.5)

R. R. Castro[1*], C. I. Huerta[1], O. Romero[2], C. Jacques[3], A. Hurtado[3] and A. I. Fernández[1]

[1]*Centro de Investigación Científica y de Educación Superior de Ensenada, División Ciencias de la Tierra, Departamento de Sismología, Ensenada, Baja California, Mexico*

[2]*Department of Geological Sciences, University of Texas, El Paso, Texas, USA*

[3]*Instituto de Geología, Universidad Nacional Autónoma de México, Estación Regional del Noroeste, Hermosillo, Sonora, Mexico*

Resumen

Analizamos ondas de cuerpo de sismos locales y regionales registrados por la Red Sísmica del Noreste de Sonora, México (RESNES) usadas para determinar funciones empíricas de atenuación para las ondas *P* y *S* que describen el decaimiento de las amplitudes espectrales a frecuencias discretas entre 0.4 y 63 Hz. Los sismos seleccionados tienen su fuente cerca de la ruptura superficial del sismo de Sonora del 3 de mayo de 1887 (M_w 7.5), ubicado en la porción sur de la provincia tectónico-fisiográfica de cuencas y cordilleras. Nuestros datos provienen de las componentes verticales y horizontales de sismogramas registrados a distancias hipocentrales de 25 a 150 km. Usamos funciones de atenuación obtenidas por Castro *et al.* (2008) con un modelo no-paramétrico invirtiendo amplitudes espectrales observadas. Las curvas de atenuación reportadas indican que las amplitudes espectrales decaen más rápido durante los primeros 40 km de las trayectorias fuente-estación y muestran otro cambio en el porcentaje de decaimiento a aproximadamente 80 km. En este artículo separamos el efecto de *Q* de la corteza superior e inferior de la atenuación total: usamos los primeros 40 km de las curvas de atenuación para estimar *Q* de la corteza superior y el segmento de 40-80 km para estimar *Q* de la corteza inferior. Encontramos que en la corteza superior la dependencia exponencial de *Q* con la frecuencia es la misma para ambas ondas *P* y *S*, específicamente $Q \sim f^{1.1}$, pero Q_S es un factor de 3 mayor, indicando que las ondas *P* experimentan mayor atenuación que las ondas *S*. En la corteza inferior *Q* es más compleja, ya que muestra una dependencia con la frecuencia más fuerte a bajas frecuencias (f < 3 Hz) y una débil dependencia con la frecuencia para las altas frecuencias (f > 6 Hz).

Palabras clave: Atenuación sísmica, Sonora, México.

Abstract

We analized body-waves of local and regional earthquakes recorded on the Seismic Network of Northeastern Sonora, Mexico (RESNES) are used to determine empirical attenuation functions for *P* and *S* waves in the interval of 0.4-63 Hz. The epicenters are near to the surface rupture of the May 3, 1887 (M_w 7.5) Bavispe, Sonora earthquake. Seismograms of vertical and horizontal components at of ground motion hypocentral distances of 25 to 150 km were used in a nonparametric model. The reported attenuation curves indicate that the spectral amplitudes decay faster in the first 40 km of the path and show different decay rate at approximately 80 km. We found that in the upper crust the exponential dependence of *Q* with frequency is the same for *P* and *S* waves, namely $Q \sim f^{1.1}$, but Q_S is larger by a factor of 3. In the lower crust *Q* is more complex, showing a strong frequency dependence below 3 Hz and a weaker frequency dependence above 6 Hz.

Key words: Seismic attenuation, Sonora, Mexico

Introduction

The Sonora earthquake of May 3, 1887 is the largest historical seismic event occurred in the southern Basin and Range province. This normal fault earthquake destroyed the town of Bavispe, and had a maximum vertical slip at the surface of 5.1 m (Suter, 2006). Based on an end-to-end rupture trace of 101.8 km, Suter (2006) estimated a moment-magnitude of M_w 7.5, in agreement with M_S =7.5 estimated by Slemmons (1977) from maximum ground displacement. Collapse of adobe structures killed about fifty persons and intensities of III on the MMI scale were observed as far south as Mexico city (Aguilera, 1920; Dubois and Smith, 1980). DuBois and Sbar (1979) estimated an average radius of felt reports of 700 km.

Seismic attenuation in the southern Basin and Range province for regional earthquakes is important for hazard evaluations. Condori (2006) and Castro *et al*. (2008) determined local and regional attenuation curves and described the decay of spectral amplitude with distance. Wich is faster near the rupture area of the 1887 earthquake compared with the surrounding region. They estimated the quality factor Q for both P and S waves using a homogeneous attenuation model.

The present paper discusses the role of seismic attenuation in the observed regional distribution of large intensities generated by the 1887 Sonora earthquake. We use local attenuation curves to study the variability of Q with depth for a two-layer model. Our model is based on the velocity model by Harder and Keller (2000) obtained from a wide-angle seismic profile near the border between Sonora and Arizona. The uppermost layer of their model consists of sedimentary and volcanic rocks. The second layer, with a thickness of 22 km, corresponds to the crystalline upper crust. The base of the lower crust (third layer) is at 38 km depth, identified as the Moho.

Data

We used a subset of the data in Condori (2006) and Castro *et al*. (2008) (Fig. 1). They used records from RESNES (Red Sísmica del Noreste de Sonora) to determine nonparametric attenuation functions (NAF) for P and S waves. Castro *et al*. (2008) had separated the data into events located northwest of the array and another with local events located in the rupture zone of the 1887 earthquake. In this paper we only use the attenuation functions obtained by Castro *et al*. (2008) from local earthquakes.

The RESNES network (Fig. 1) monitors the three major normal faults that ruptured during the 1887 earthquake: Pitáycachi, Teras, and Otates at north, central, and southern segments of the rupture. The RESNES network consists of nine digital four-component stations (Castro *et al*., 2002; Romero *et al*., 2004; Castro *et al*., 2008). For epicentral location some stations from the NARS-Baja (Trampert *et al*., 2003) and RESBAN arrays located in Sonora are also used. Fig. 2 shows a 3-component acceleration record,
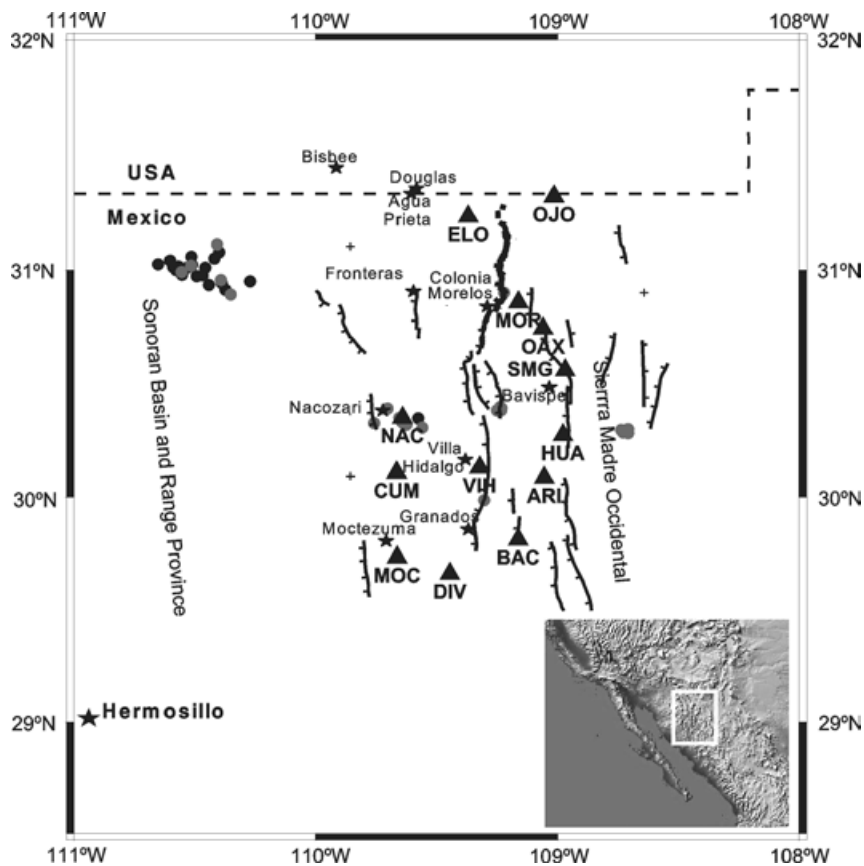

Fig. 1. Map of northeastern Sonora, modified from Castro *et al*. (2008), that shows the distribution of the stations (triangles) of the seismic network RESNES and epicenters (circles) of earthquakes located near the faulting area of the 1887 earthquake and used in this study. The lines are faults and the thicker line the trace of the 1887 surface rupture taken from Suter and Contreras (2002).
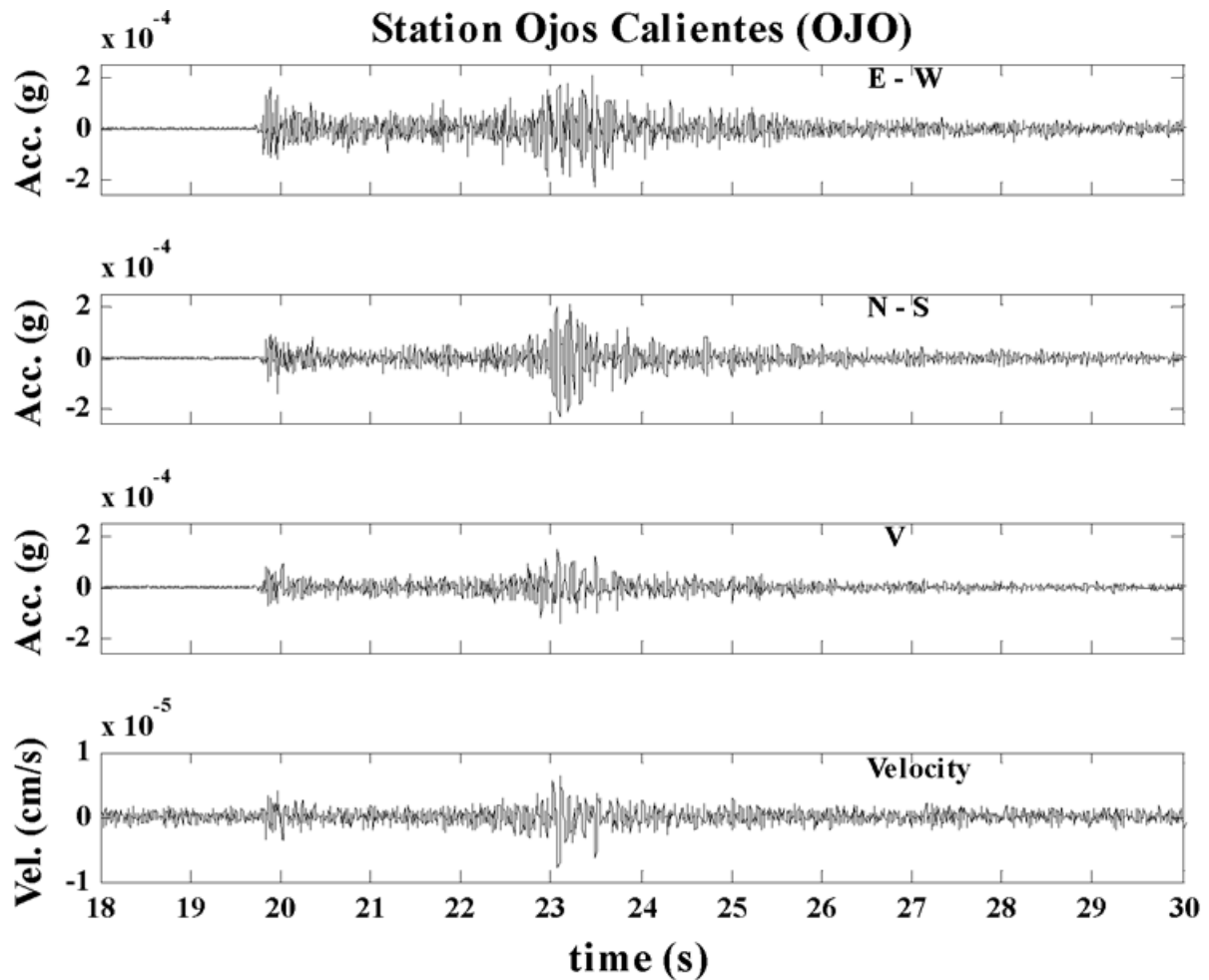
Fig. 2. Accelerogram recorded at station Ojos Calientes from a local earthquake located at about 26 km from the station. Three components of ground acceleration and a velocity component are displayed, from top frame to bottom: east-west, north-south, and vertical acceleration components, and vertical velocity component.

and the vertical component of ground velocity, from a local earthquake recorded at Ojos Calientes, located at the northern end of the array, next to the Mexico-US border.

The data set used by Castro *et al.* (2008) included earthquakes with hypocentral distances between 25 and 150 km and coda-magnitudes between 1.8 and 3.2. Regional attenuation curves were obtained from events with hypocentral distances greater than 100 km as measured from the center of the network. Local NAF were found for earthquakes located near the fault zone that ruptured in 1887, within a radius of 100 km from the center of the network. These empirical attenuation functions describe spectral amplitude decay at 23 different frequencies between 0.4 and 63.1 Hz.

In this paper we use the NAF reported by Castro *et al*. (2008) in the region of the 1887 earthquake. Fig. 3 shows a sample of these attenuation functions for 8 different frequencies between 1 and 50 Hz for *P* (solid lines) and *S* waves (dashed lines). Note that the rate of amplitude decay with distance is not constant. However, at about 80 km the decay functions become approximately constant with distance, probably due to less severe geometrical spreading. At short distances (r < 40 km), the ray-paths sample the shallow part of the crust and the spectral amplitudes decay faster than at longer distances, suggesting higher attenuation at shallow depths.

Method

We model the first 40 km of the NAF as a product of three functions representing different attenuation mechanisms

$$A(f, r) = G(r) \cdot e^{-\pi f R / vQ} \cdot e^{-\pi f Ko} \quad (1)$$

where *A(f,r)* represents the attenuation curve at hypocentral distance *r* and at a fixed frequency *f*. The first right-hand term accounts for geometrical spreading, the second term for amplitude decrease due to total *Q* (intrinsic plus scattering *Q*), and the third term for near-surface attenuation. The parameter *v* is the average wave velocity in the upper crust, 3.23 km/s for *S* waves and 5.75 km/s for *P* waves. These average velocities were taken from Harder and Keller (2000). Based on their velocity model, we estimate that source-station paths in the distance range *r*≤ 40 km sample the upper 23-25 km of the crust. In equation (1) *R=(r-10)* and *Ko* is the average decay parameter.

The geometrical spreading function is approximated as

$$G(r) = \begin{cases} 10/r & , \quad r < r' \\ 10/(r'r)^{1/2} & , \quad r \geq r' \end{cases} \quad (2)$$

where *r'* is the distance at which the geometrical spreading starts having less effect upon the amplitude decay. We find *r'*=80 km based on the change of rate of amplitude decay in the attenuation functions (Fig. 3). This distance also marks the transition between body-wave and surface-wave geometrical spreading. In many regions this transition starts near 100 km, but Fig. 3 suggests that in northeastern Sonora the geometrical spreading transition may begin at a shorter distance range. Equations (1) and (2) are normalized at 10 km, the minimum source-station distance recorded by RESNES (see Fig. 2 in Castro *et al.*, 2008). To determine the NAF, Castro *et al.*, (2008) used acceleration spectra from selected events at hypocentral distances between 25 and 150 km. They assumed that at *r* = 0 there is not attenuation; consequently the attenuation functions were constrained to cross the origin. Thus, the NAF describe the spectral amplitude decay within the 0-150 km range (Fig. 3).
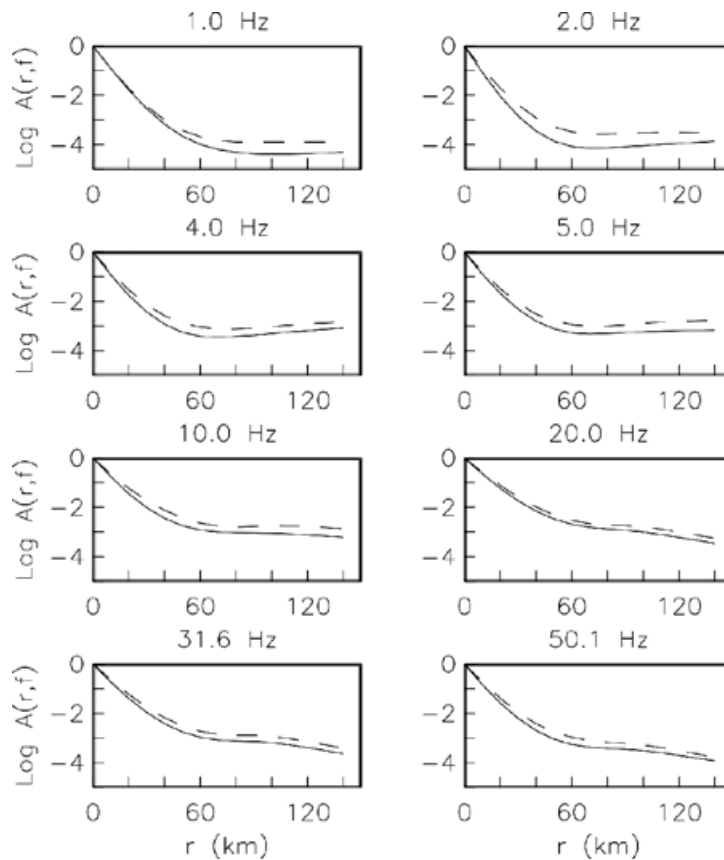

Fig. 3. Nonparametric attenuation functions (NAF) determined by Castro *et al.* (2008) using local earthquakes recorded by RESNES near the 1887 rupture zone. Solid and dashed lines are the NAF determined using *P* and *S* waves, respectively.

Parameters Q and Ko may be estimated at each frequency by taking the logarithms of both sides of equation (1):

$$a(R) = mR + b \qquad (3)$$

where $a(R) = log\,A(f,r) - logG(r)$, $m = -\pi f\,log\,e\,/Q\,v$, and $b = -\pi f\,log\,eKo$. The slope m is estimated by a least square fit of equation (3). For a given frequency f, Q can be estimated as

$$Q(f) = \frac{\pi f \log e}{mv} \qquad (4)$$

and

$$Ko(f) = \frac{b}{\pi f \log e} \qquad (5)$$

Attenuation in the lower crust was obtained by correcting the original NAF for upper crust attenuation using the values of $Q(f)$ and $Ko(f)$ estimated from equations (4) and (5). We used the 40-80 km segment of the corrected NAF to estimate total Q in the lower crust from the parametric model

$$A_l(f,r) = \frac{1}{r^b}\exp-\left[\frac{\pi f r}{Q_2 v_2}\right] \qquad (6)$$

where $A_l(f,r)$ are the amplitudes of the NAF corrected for upper crust attenuation, including near surface attenuation. We used an average velocity (v_2) of 6.6 and 3.7 km/s for P and S waves, respectively, after Harder and Keller (2000). Q_2 is the sum of intrinsic and scattering Q in the lower crust. We linearize equation (6) by taking logarithms and we search for values of b and Q_2 that yield the best least-squares solution for each frequency considered (*e.g.* Castro *et al.*, 2004). We estimate that the 40-80 km segment of the NAF yields the attenuation in the lower crust; thus we are sampling down to approximately 50 km depth.

Results and Discussion

A comparison between P- and S-wave NAF (Fig. 3) suggests that P waves may be more strongly attenuated than S waves. This observation agrees with the estimates of total Q from the 2-layer model described above. From equations (1) and (6) and the trade-off between geometrical spreading and Q, our Q estimates depend on the definition of geometrical spreading adopted. Also, our estimates of Q are based on the observed rate of amplitude decay represented by the NAF (Eq. 4), wich may be influenced by factors unrelated to attenuation. Thus in the 60-100 km range some postcritical reflections may influence the spectral amplitude decay, although we selected time windows containing mainly direct arrivals to calculate the acceleration spectra.

Fig. 4 shows the estimates of Q for the upper and lower crust ($Q > 0$), and the Q-frequency relations from a least-squares fit of the Q estimates. We were able to make estimates of Q_P in the frequency band 0.6-63 Hz and for Q_S between 1.0 Hz and 63 Hz. Fig. 4 shows estimates of Q for P waves (triangles) and for S waves (squares). In the upper crust (left frame) the exponential dependence of Q with frequency is the same for both, waves namely $Q \sim f^{1.1}$, but Q is higher by a factor of 3 for P compared with S waves. In the lower crust (right frame) the frequency dependence of Q is more complicated and differs for P and S waves. In general, the frequency dependence of Q is stronger at low frequencies. At high frequencies, $f > 7$ Hz, Q_P is approximately constant, while Q_S remains frequency dependent. It is interesting that, as in the upper crust, P waves attenuate more strongly than S waves in the lower crust as a result of scattering and intrinsic Q. In the lower crust $Q_P < 0$ between 2.5 and 5.0 Hz for values of the geometrical spreading exponent b close to 1.0 (Fig. 5). For this frequency band P-wave geometrical spreading must be less severe (b smaller than 1.0), but the trade-off between Q and b yields a better solution for $Q < 0$. Fig. 5 shows the exponent b in equation (6) as a function of frequency for P (triangles) and S (squares). In general the exponent $b < 1.0$. between 2 and 20 Hz b for S waves takes values close to 0.8.

The possible cause of the dependence of Q with frequency has been debated by different authors (Knopoff, 1964; Tsai and Aki, 1969; Aki and Chouet, 1975; Rautian and Khalturin, 1978; Aki, 1980; among others). Aki and Chouet (1975), suggested that the apparent frequency dependence of coda Q may be due to strong changes of Q with depth. The frequency dependence of Q has been also related to tectonic activity. For instance, Aki (1980) observed that in Hawaii, Q increases only slightly with frequency and is lower than in other areas. Under the Kilauea, Ellsworth (1977) observed a weaker heterogeneity in the mantle and this may cause less efficient body-wave scattering and also may explain the weak dependence of Q with frequency. In this volcanic region the ductility associated with the presence of magma and the high temperature could reduce small-scale heterogeneities that generate seismic wave scattering (Aki, 1980).

The southern Basin and Range in Sonora is a tectonic region under extension. High temperatures in the lower crust may play a role by reducing high-frequency scattering and caussing a weaker frequency dependence of Q, as in Fig. 4. Tectonic extension and magmatism in the Basin and Range province has generated an increase in surface heat flow relative to other more stable tectonic provinces such as the Colorado Plateau (Parsons, 1995).

The increased heat flow may be caused by lithospheric thinning (*e.g.* Crough and Thompson, 1976; Lachenbruch and Sass, 1978; Artyushkov and Batsanin, 1984). In contrast, in the upper crust, near the rupture zone of the 1887 Sonora earthquake, the presence of faults and the highly fractured rocks can generate strong body-wave scattering and lower Q. Comparing the values of total Q between upper and lower crust (Fig. 4), it is clear that attenuation is stronger in the upper crust. The implication is that seismic waves arriving at epicentral distances larger than 40 km will have less attenuated amplitudes because the rays will tend to travel along the lower crust, where Q is higher. This may help explain why, the felt intensity generated by the 1887 earthquake extended as far as it did. DuBois and Sbar (1979) estimated that the average radius of felt reports was about 700 km. These results also illustrate the important role played by the values of Q in the crust.
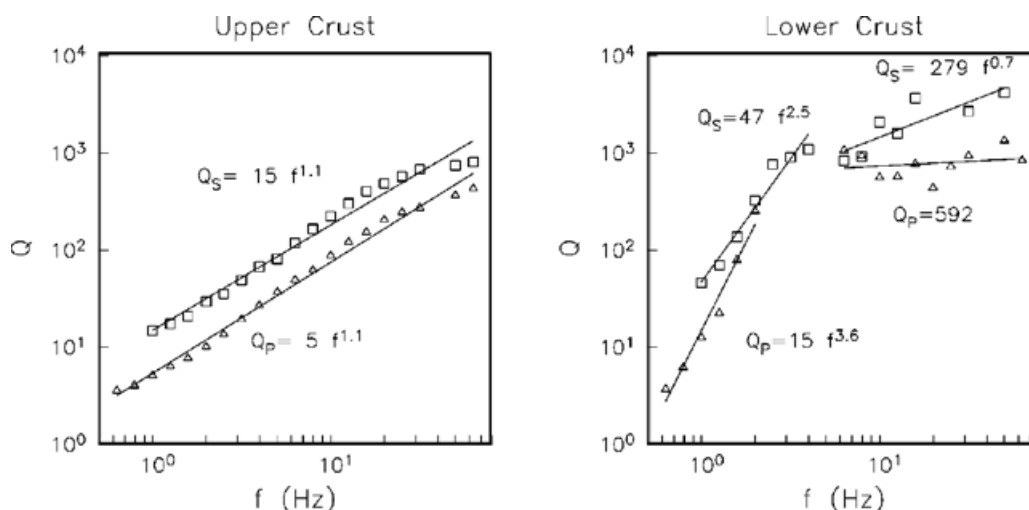

Fig. 4. Total Q estimated using a 2-layer model. Left frame correspond to the first 23-25 km of the crust and the right frame to the next 25 km. Triangles correspond to P waves (Q_P) and squares to S waves (Q_S). The lines are the least-squares fit obtained with the estimates of Q shown.
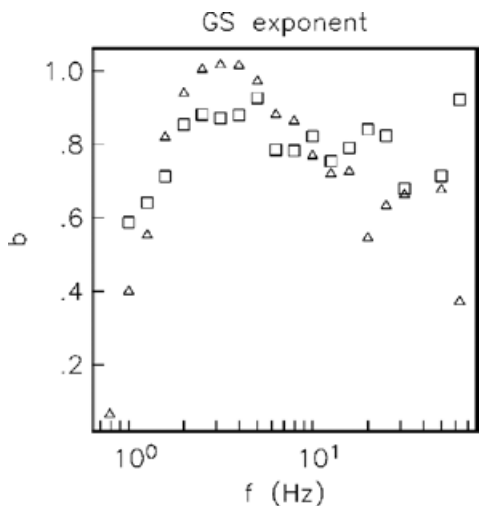

Fig. 5. Values of the exponent b (Eq. 6) obtained for P (triangles) and S (squares) waves.

Conclusions

The NAF curves and the estimates of total Q obtained for the crust indicate that P waves attenuate more than S waves near the rupture zone of the 1887 Sonora earthquake. Source-station rays traveling in the lower crust attenuate less, due to a less severe scattering and internal friction, than rays that propagate in the upper crust. Consequently, at short epicentral distances the intensities attenuate faster than at intermediate ($r > 40$ km) and regional ($r > 100$ km) distances. Finally, the weaker high-frequency dependence of Q observed in the lower crust may be due to the ductility of the deeper rocks and high temperature that reduces small-scale heterogeneities.

Bibliography

Aguilera, J. G., 1920. The Sonora earthquake of 1887, *Bull. Seism. Soc. Am. 10*, 5-56.

Aki, K. and B. Chouet, 1975. Origin of coda waves: source, attenuation and scattering effects, *J. Geophys. Res. 80*, 3322-3342.

Aki, K., 1980. Scattering and attenuation of shear waves in the lithosphere, *J. Geophys. Res. 85*, 6496-6504.

Artyushkov, Y. V. and S. F. Batsanin, 1984. Change in the thermal regime of the Eartht's crust associated with the approach of anomalous mantle to its lower boundary, *Izvestiya, Earth Physics*, *20*, 887-891.

Castro, R. R., O. M. Romero and M. Suter, 2002. Red sísmica para el monitoreo de la sismicidad del sistema de fallas normales del noreste de Sonora, *GEOS 22*, 379.

Castro, R. R., M. R. Gallipoli and M. Mucciarelli, 2004. An attenuation study in southern Italy using local and regional earthquakes recorded by the seismic network of Basilicata, *Ann. Geofisica 47*, 1597-1608.

Castro, R. R., C. Condori, O. Romero, C. Jacques and M. Suter, 2008. Seismic attenuation in northeastern Sonora, Mexico, *Bull. Seism. Soc. Am. 98*, 722-732.

Condori, C., 2006. Estudio de atenuación sísmica de la región noreste de Sonora, Tesis de Maestría, División Ciencias de la Tierra, CICESE, 88pp.

Crough, S. T. and G. A. Thompson, 1976. Thermal model of continental lithosphere, *J. Geophys. Res.*, *81*, 4857-4862.

DuBois, S. and M. L. Sbar, 1979. The northern Sonora earthquake of 1887: hazard implications for Arizona, *Geol. Soc. Am. Abstracts with Programs 11*, 416.

DuBois, S. and A. W. Smith, 1980. The 1887 earthquake in San Bernardino Valley, Sonora, *State of Arizona, Bureau of Geology and Mineral Technology, Special Paper 3*, 112pp.

Ellsworth, W. L. 1977. Three-dimensional structure of the crust and mantle beneath the island of Hawaii, Ph.D. thesis, 327 pp., Mass. Inst. of Technol., Cambridge.

Harder, S. and G. R. Keller, 2000. Crustal structure determined from a new wide-angle seismic profile in southwestern New Mexico, *New Mexico Geol. Soc. Guidebook 51*, 75-78.

Knopoff, L., 1964. Q *Rev. Geophys. 2*, 625-660.

Lachenbruch, A. H. and J. H. Sass, 1978. Models of an extending lithosphere and heat flow in the Basin and Range province, *in Cenozoic tectonics and regional geophysics of the western Cordillera*, Smith, R. B. and G. P. Eaton (Editors), *Geol. Soc. Am. Mem. 152*, 209-250

Parsons, T., 1995. The Basin and Range province, *in Continental Rifts: Evolution, Structure, Tectonics*, K.H. Olsen (Editor), Elsevier, Amsterdam, 277-324

Rautian, T. G. and V. I. Khalturin, 1978. The use of coda for determination of the earthquake source spectrum, *Bull. Seism. Soc. Am. 68*, 923-948.

Romero, O. M., C. Jacques and R. R. Castro, 2004. Análisis de la sismicidad detectada por la red sismológica del noreste de Sonora, *GEOS 24*, 230.

Slemmons, D., 1977. State of the art for assessing earthquake hazards in the United Status: faults and earthquake magnitude, *Rep. 6, U.S. Army Waterways Expt. Station*, Vicksburg, Mississippi, 129 pp.

Suter, M. and J. Contreras, 2002. Active tectonics of northeastern Sonora, Mexico (southern Basin and Range province) and the 3 May 1887 M_w 7.4 earthquake, *Bull. Seism. Soc. Am. 92*, 581-589.

Suter, M., 2006. Contemporary studies of the 3 May 1887 M_w 7.5 Sonora, Mexico (Basin and Range Province) earthquake, *Seism. Res. Lett. 77*, 134-147.

Trampert, J., H. Paulsen, A. Van Wettum, J. Ritsema, R. Clayton, R. Castro*,* C. Rebollar and A. Pérez-Vertti, 2003. New array monitors seismic activity near the Gulf of California in México, *EOS, Trans. Am. Geoph. Union 84*, 29-32.

Tsai, Y. B. and K. Aki, 1969. Simultaneous determination of seismic moment and attenuation of seismic surface waves, *Bull. Seismol. Soc. Am. 59*, 275-287.

R. R. Castro[1*], C. I. Huerta[1], O. Romero[2], C. Jacques[3], A. Hurtado[3] and A. I. Fernández[1]
[1]Centro de Investigación Científica y de Educación Superior de Ensenada, División Ciencias de la Tierra, Departamento de Sismología, km 107 Carretera Tijuana-Ensenada, 22860 Ensenada, Baja California, Mexico,
[2]Department of Geological Sciences, University of Texas, El Paso, TX79968-0555
[3]Instituto de Geología, Universidad Nacional Autónoma de México, Estación Regional del Noroeste, A. P. 1039, 83000 Hermosillo, Sonora, Mexico
**Corresponding author: raul@cicese.mx*